Research Square

Preprints are preliminary reports that have not undergone peer review.
They should not be considered conclusive, used to inform clinical practice,
or referenced by the media as validated information.

Air pollution imposes an unseen compound burden on outdoor thermal comfort across India

Subrahmanya Hari Prasad Peri

pshari19@gmail.com

Indian Institute of Technology

A. N. V. Satyanarayana

Indian Institute of Technology

Article

Keywords: Air Pollution, UTCI, MECI, Heat Exposure, ERA5, CPCB

Posted Date: November 3rd, 2026

DOI: https://doi.org/10.21203/rs.3.rs-11548795/v1

License: This work is licensed under a Creative Commons Attribution 4.0 International License.
Read Full License

Additional Declarations: No competing interests reported.

Air pollution imposes an unseen compound burden on outdoor thermal comfort across India

Peri Subrahmanya Hari Prasad[1,*] and **A. N. V. Satyanarayana**[1]

[1]Centre for Oceans, Rivers, Atmosphere and Land Sciences (CORAL), Indian Institute of Technology Kharagpur, Kharagpur 721302, West Bengal, India

[*]Correspondence: pshari19@gmail.com

Abstract

Air pollution and thermal stress are experienced together but assessed separately. Here we quantify modelled pollution-related shifts in outdoor thermal comfort across Indian states during 2016–2023, using 423 regulatory monitoring stations and reanalysis-based UTCI. At monthly state scale, pollutant anomalies show no statistically detectable association with UTCI anomalies after accounting for seasonality, consistent with nonlinear machine-learning results. A published index integrating both dimensions fails on transfer to India, producing unphysical comfort gains in clean regions. We therefore recalibrate it with Indian regulatory anchors. The recalibrated index estimates winter and post-monsoon comfort-index shifts concentrated across the Indo-Gangetic Plain, reaching 4 °C-equivalent in Delhi. A population-weighted dual-exposure classification shows 2.98 billion person-months of model-defined compound exposure each year, two-thirds of India's thermal-stress burden. This burden is invisible to thermal indices, and to the separate frameworks that currently govern heat and air quality.

Keywords: Air Pollution; UTCI; MECI; Heat Exposure; ERA5; CPCB

Introduction

Climate hazards increasingly arrive in combination rather than in isolation, and the recognition that compound events — multiple drivers or hazards whose joint occurrence amplifies impact — constitute a distinct scientific object has reorganised both climate science and environmental epidemiology over the past decade.[1–3] Public-health syntheses now treat compound climate exposures as a frontier in their own right, with interactions between heat and air pollution identified as the pairing with the deepest evidence base and the largest exposed populations.[4,5] Multi-country analyses show that compound extreme-temperature–PM2.5 events have increased in frequency, duration and spatial extent, with the burden concentrating in rapidly urbanising regions;[6] projections indicate steep growth of humid-heat exposure through this century;[7] and modelling of future heatwave–ozone co-occurrence anticipates that climate change will distribute these compound episodes inequitably across populations.[8]

The epidemiological case that joint exposure is worse than the sum of its parts has hardened considerably. Systematic reviews of pollution–temperature–pollen interactions find consistent synergy across designs and outcomes,[9,10] and classic multi-city work showed heatwave mortality to be modified substantially by concurrent air-pollution levels.[11] Recent studies document synergistic effects of high temperature and pollution on mortality in Northeast Asia,[12] temperature modification of ozone–mortality relationships across China,[13] elevated myocardial-infarction mortality under joint temperature–PM2.5 extremes,[14,15] spatially heterogeneous synergy of heat and smoke on cardiorespiratory hospitalisations,[16] additive-interaction excess mortality under co-occurring PM2.5 and extreme heat in British Columbia,[17] and compound heat–pollution effects on child hospitalisations across five countries.[18] In parallel, atmospheric analyses established that extremes of ozone, particulate matter and temperature co-occur far more often than chance,[19,20] and that cities act as persistent hotspots of compound heat and fine-particulate pollution relative to their rural surroundings.[21,22]

India concentrates every element of this problem. Heatwaves are well characterised, intensifying, and a recognised public-health hazard,[23–26] thermal stress over the northwest has been rising for decades,[27] and surface temperatures are projected to continue climbing,[28] with the health–climate nexus in Indian cities repeatedly flagged as critically under-governed.[29,30] Simultaneously, India carries the world's heaviest particulate burden: long-term reconstructions document the evolution of PM2.5 since 1998,[31] satellite-

based databases resolve its two-decade spatial structure,[32] and short-term PM2.5 exposure is directly associated with daily mortality in Delhi.[33] The National Clean Air Programme (NCAP) has begun to alter these trajectories,[34,35] but progress is uneven across cities and seasons,[36,37] and recent high-resolution assessments reveal inequalities in who has benefited from the improvement.[38] Most pertinently, the compound dimension has entered Indian research almost exclusively in one causal direction — heat amplifying pollution — exemplified by the recent demonstration that heatwaves trigger severe surface-ozone episodes nationwide, with ozone remaining elevated for days after heatwave cessation and substantial attributed health burden,[39] alongside evidence of ozone's growing exposure and economic cost in India[40] and of heatwave impacts on multiple pollutants across climatic zones.[41]

The reverse direction — what pollution does to the thermal environment that people actually experience — runs through the apparatus of outdoor thermal comfort. From the early discomfort index[42] through the physiological equivalent temperature[43] to the Universal Thermal Climate Index (UTCI), built on a multi-node model of human thermoregulation[44,45] and benchmarked against alternative indices,[46] biometeorology has refined how meteorology is translated into physiological strain, and reanalysis-based products now provide global, validated UTCI fields.[47,48] Indian applications of this apparatus are growing, from city- and park-scale comfort assessments to local-climate-zone analyses.[49–51] Yet every index in this lineage is a function of meteorology alone. Evidence that this omits something real has accumulated from three methodologically distinct directions: radiative-transfer modelling shows aerosol loading altering physiological equivalent temperature through its control of direct and diffuse radiation;[52] field campaigns find thermal, air-quality and respiratory comfort votes degrading with PM2.5, most strongly at thermal extremes;[53] and machine-learning attribution across hundreds of Chinese cities detects systematic, season- and daytime-dependent pollutant–UTCI associations.[54] The one formal integration of the two dimensions — the Meteorology and Environment Comfort Index (MECI), which superimposes Fechner-law pollutant terms,[55–57] grounded in the psychophysics of logarithmic perception,[58] on a somatosensory temperature — was developed and applied in five Chinese cities,[55] and statistical couplings of urban thermal dynamics with pollution have since been demonstrated for Delhi.[59] This literature, however, leaves three gaps that together motivate the present study. First, the integrated-index strand has remained descriptive and small in scale — a handful of cities, percentages of hours by comfort class, no uncertainty quantification — while the association strand[53,54] has remained index-free, estimating statistical couplings without producing an exposure metric that planning can use. Second, the two strands have never been confronted with one another: whether the associations detected in raw data survive the removal of shared seasonality — and hence whether a thermal index could even in principle absorb pollution information — is an open statistical question with direct consequences for how compound exposure must be constructed. Third, whether a perception-based index transfers beyond the pollution climate in which it was calibrated has never been examined; transfer failures of this kind are silent, producing plausible-looking numbers rather than errors, and can only be caught by testing the index against an environment spanning a wider concentration range than its calibration domain.

Here we quantify modelled pollution-related changes in outdoor thermal comfort across Indian states over 2016–2023, combining 423 regulatory monitoring stations with reanalysis-based UTCI, and we close each of these gaps with an analysis chain designed so that every stage motivates the next. We first establish the observational setting with quality-controlled trend analysis — seasonal Mann–Kendall tests and Sen's slopes, supplemented by a fixed-station sensitivity analysis of monitoring-network expansion — showing that particulates declined through the NCAP era without a detectable UTCI trend over this interval. We then test the association question at three levels of statistical stringency — deseasonalised correlation structure, two-way fixed-effects panel models with cluster-robust inference, and gradient-boosted machine-learning attribution validated out-of-state — and find that there is no statistically detectable residual pollution–UTCI association at monthly scale in the tested models. Turning to the integrated index, we demonstrate that the published MECI calibration fails on transfer to India, generating unphysical comfort gains in clean states, and derive an India-calibrated formulation anchored to national regulatory breakpoints, with its somatosensory-temperature calculation checked against published reference values and propagated throughout with bootstrap uncertainty quantification. The recalibrated index reveals a sharply seasonal geography of pollution-driven comfort loss centred on the Indo-Gangetic Plain, and a statistical persistence projection indicates how that geography would evolve to 2030 under continuing trends. Finally, because the blindness result implies that compound exposure cannot be inferred from either hazard alone, we construct a dual-exposure classification joining UTCI thermal tiers to the regulatory pollution term, and

weight it with gridded population: compound exposure occupies nearly half of all months in the worst-affected states and totals 2.98 billion person-months per year nationally — two-thirds of India's thermal-stress exposure carrying a concurrent pollution load invisible to thermal assessment — a burden aligned specifically with state-level SDG 13 climate-action performance, and one that no operational index currently sees.

Results

Divergent trajectories of air pollution and the thermal environment

We first characterised the 2016–2023 trajectories of the four criteria pollutants and of the thermal environment across the 14-state trend cohort (states with ≥60% monthly PM2.5 coverage beginning no later than 2017; Methods). PM2.5 declined significantly (seasonal Mann–Kendall, $p < 0.05$) in nine of the 14 states, with no state showing a significant increase (Fig. 1a, b). The steepest declines occurred in Uttar Pradesh (−9.38 μg m^{-3} yr^{-1}, $p < 0.001$), Odisha (−5.62 μg m^{-3} yr^{-1}), Tamil Nadu (−5.19 μg m^{-3} yr^{-1}) and Delhi (−4.49 μg m^{-3} yr^{-1}), with a cohort-median Sen's slope of −1.67 μg m^{-3} yr^{-1}. PM10 (seven states declining, two increasing; median −2.00 μg m^{-3} yr^{-1}) and NO_2 (eight declining, three increasing) followed similar trajectories, whereas SO_2 showed no coherent direction (three declining, five increasing; median −0.06 μg m^{-3} yr^{-1}). Monitoring-network expansion was examined in a fixed-station sensitivity check: slopes recomputed using only the 61 stations reporting continuously from 2017 or earlier showed broadly concordant trend directions, with exceptions across states.

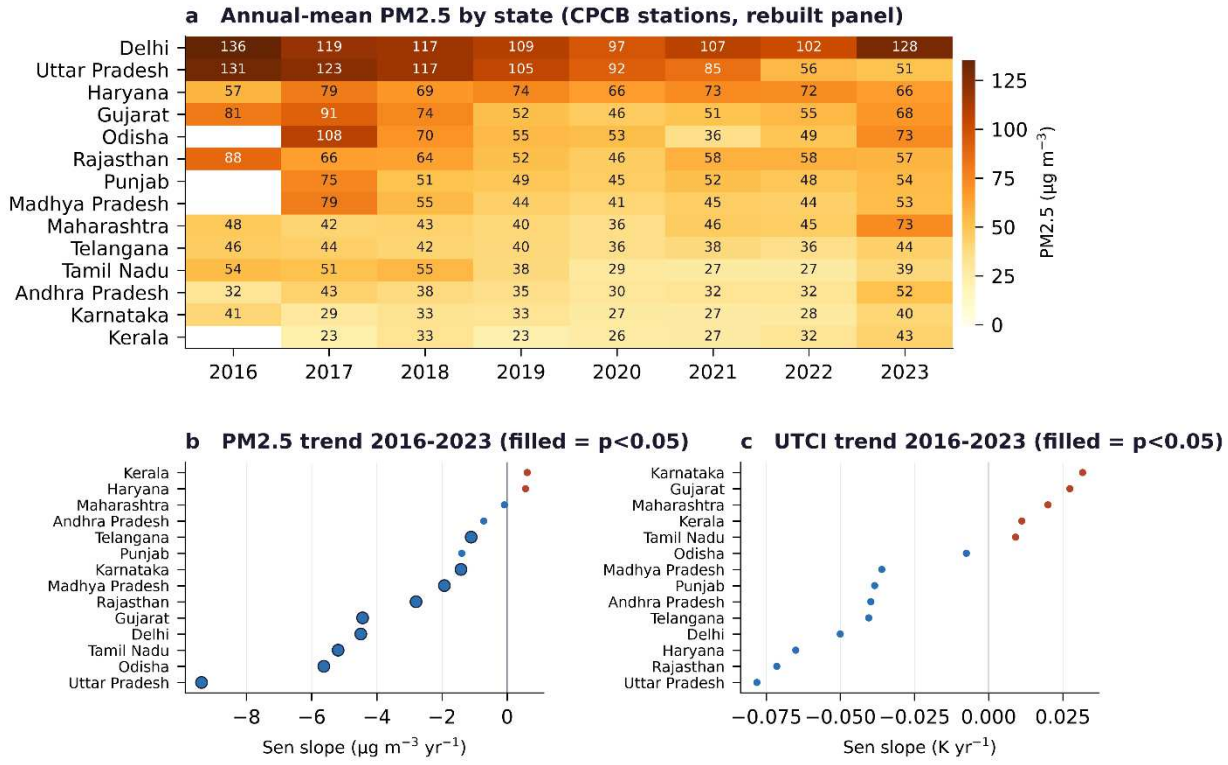


Figure 1 Trends in air pollution and the thermal environment across Indian states, 2016–2023. ***a***, *Annual-mean PM2.5 by state for the 14-state trend cohort, from the rebuilt Central Pollution Control Board (CPCB) station panel (state value = median across stations after quality control; Methods).* ***b***, ***c***, *Sen's slopes from the seasonal Mann–Kendall test for PM2.5 (**b**) and monthly-mean UTCI (**c**); filled markers denote $p < 0.05$, blue declining and red increasing trends. The year 2024 is excluded throughout owing to incomplete source data (Methods).*

The thermal environment showed no comparable trajectory. Over the same window, no state exhibited a significant trend in monthly-mean UTCI (cohort median −0.04 K yr^{-1}; Fig. 1c), and air temperature trends were likewise indistinguishable from zero in all but one state. The 2016–2023 window is too short to resolve

climate-scale warming; what it establishes here is a descriptive contrast—pollution trends during the regulatory intervention period without a detectable UTCI trend over the same interval—which frames the central question of this study: whether indices of outdoor thermal comfort register any part of the changing pollution burden.

No detectable pollution–UTCI association at monthly scale

Raw seasonal associations between UTCI and pollutant concentrations appear strong but largely reflect shared seasonality. In the post-monsoon season, when atmospheric stagnation coincides with falling temperatures, raw rank correlations reach r = −0.80 (PM10) and −0.77 (PM2.5), and in winter −0.57, while the monsoon washout season shows the opposite sign (+0.32 to +0.34; Fig. 2a). Once state–month climatology is removed, these associations collapse: the largest surviving anomaly correlation is r = −0.21 (PM2.5, monsoon; Fig. 2b). A two-way fixed-effects panel model with year effects and cluster-robust errors does not detect a significant residual association: a +10 μg m^{-3} PM2.5 anomaly is associated with a UTCI change of +0.026 K (95% CI −0.018 to +0.071, p = 0.22, n = 1,108 state-months), with no season individually significant (seasonal coefficients −0.036 to +0.060 K, all p > 0.17). The nonlinear prediction test gives a consistent result: a gradient-boosted model validated out-of-state found no out-of-state predictive gain from pollutant anomalies — adding them *reduced* cross-validated R^2 from 0.35 to 0.11 (ΔR^2 = −0.25), with per-pollutant permutation importances indistinguishable from zero (Supplementary Fig. S1).

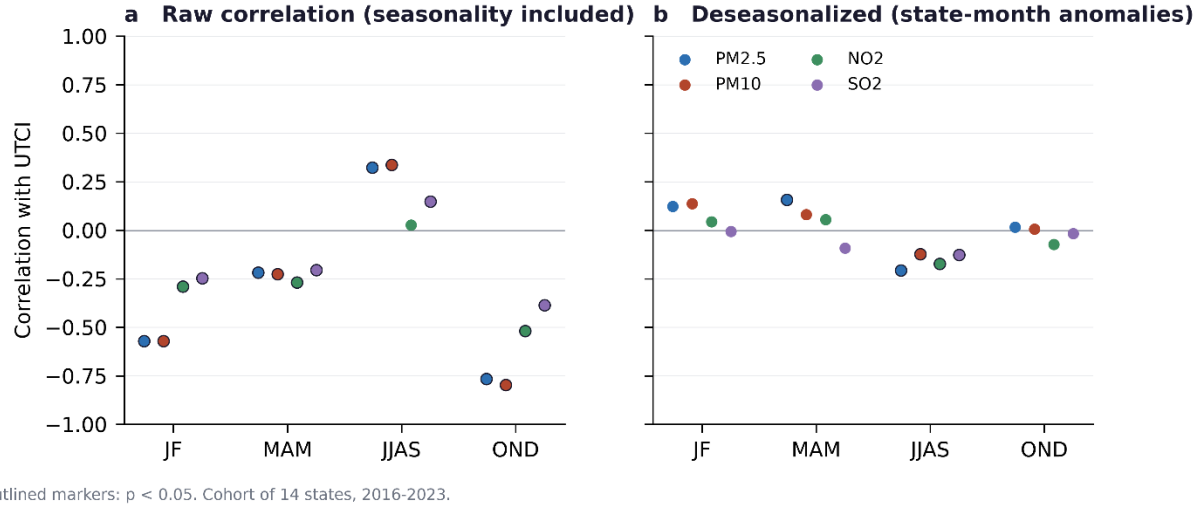


Figure 2 Apparent UTCI–pollution associations are seasonal artefacts. ***a****, Spearman rank correlations between monthly-mean UTCI and four pollutants by IMD season (Winter JF, Pre-monsoon MAM, Monsoon JJAS, Post-monsoon OND), computed on raw values for the 14-state cohort, 2016–2023.* ***b****, The same associations computed on state–month anomalies, which remove seasonality and fixed geography. Outlined markers denote p < 0.05.*

What the biometeorological index does describe is geography and season. Across all 32 states (3,032 state-months, 2016–2023), 69.3% of monthly means fall in the UTCI no-thermal-stress band (9–26 °C), 9.5% in moderate heat stress and 21.2% on the cold side, the latter dominated by the Himalayan states (Fig. 3a, b). The annual-cycle envelope spans more than 55 °C between the warmest (Puducherry) and coldest (Jammu & Kashmir, an area average including high-Himalayan terrain) state climatologies (Fig. 3c). Monthly averaging, however, compresses extremes — no monthly-mean UTCI exceeds 28.4 °C, so classes above moderate heat stress are structurally invisible at this resolution (Methods). Together, Figs. 2 and 3 establish the premise for what follows: UTCI resolves India's thermal geography but does not explicitly encode the co-occurring pollution burden, so a combined exposure must be represented explicitly rather than inferred from thermal variables.

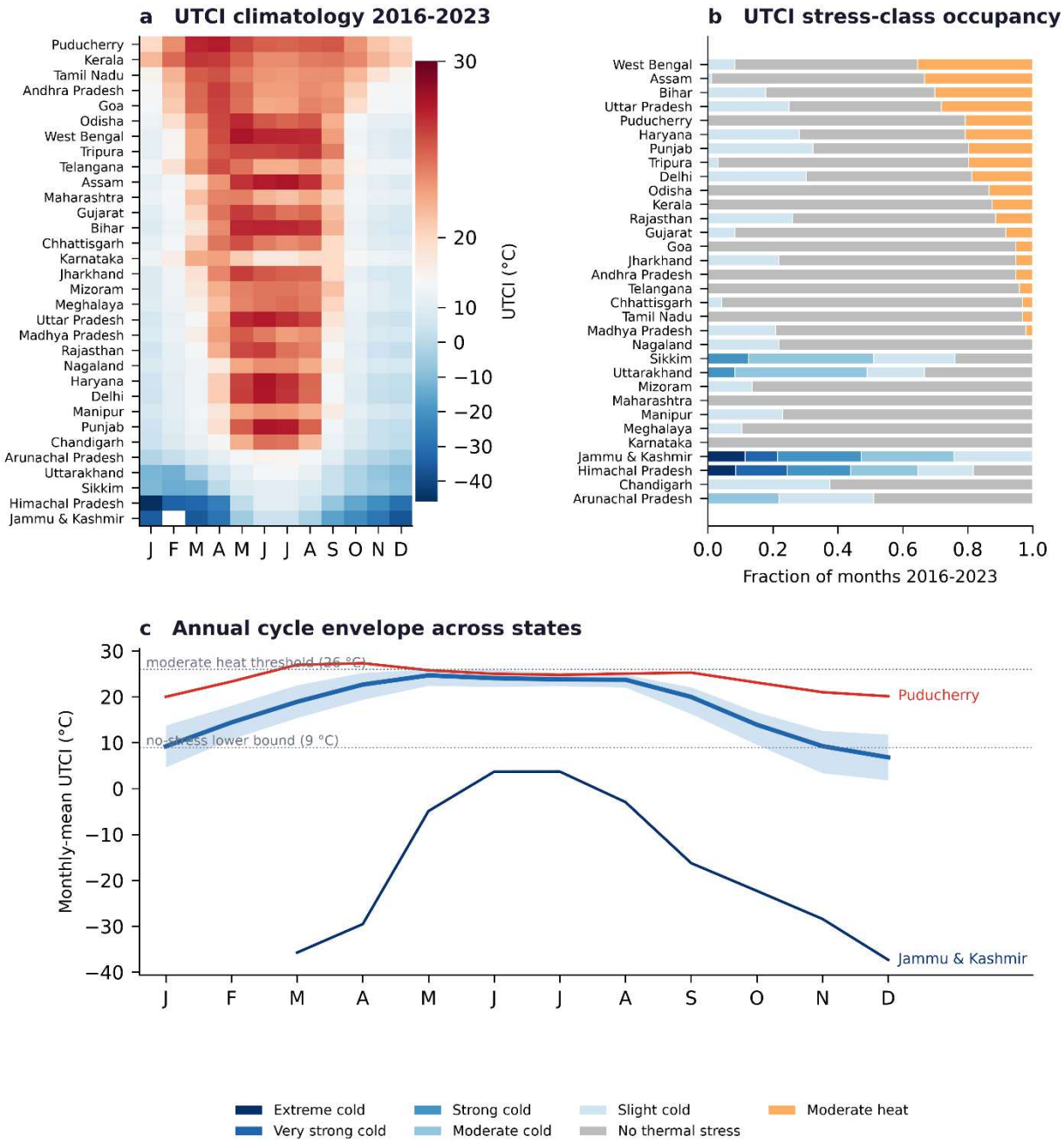


Figure 3 The biometeorological baseline of India, 2016–2023. ***a***, *Climatological monthly-mean UTCI by state and calendar month (diverging scale centred on the no-stress band midpoint, 17.5 °C; white cells, quality-masked).* ***b***, *Fraction of state-months in each UTCI thermal-stress class; classes above moderate heat are unreachable at monthly resolution.* ***c***, *Median and interquartile range of the 32 state climatologies, with the warmest and coldest states labelled; dotted lines mark the no-stress band bounds (9 °C, 26 °C).*

Naïve transfer of the Fechner calibration fails; an India-calibrated index

Applying the published MECI formulation directly to Indian conditions produced physically meaningless results, for a reason intrinsic to its construction. The relaxation coefficients of the original index are Fechner-law fits anchored between the WHO-2005 guideline and its nearest interim target, with the perceived-pollution sensation L calibrated only on that interval. Below the lower anchor the logarithmic term extrapolates without bound: at concentrations typical of India's clean northeastern and Himalayan states

(for example PM2.5 of 15 μg m⁻³), each pollutant contributes a *negative* sensation (rc = −1.26 for PM2.5 alone), and the four terms sum to comfort "bonuses" of 10–15 °C-equivalent — clean air emerging as a larger thermal intervention than severe pollution. The original study could not have encountered this regime, because none of its five Chinese cities sampled sub-guideline air. Transfer of the index to any region with clean-air monitoring therefore requires recalibration.

We recalibrated the relaxation coefficients with Indian regulatory anchors: L = 0 at the CPCB Air Quality Index "Satisfactory" bound — which coincides with the NAAQS 24-h standard but is applied here to monthly means — and L = 1 at the next CPCB breakpoint, with rc floored at zero below the anchor so that concentrations below the reference anchor yield zero modelled relaxation rather than a benefit (Methods; Supplementary Table S1 reports the derived coefficients). The accompanying somatosensory-temperature formulation was validated by reproducing the published mean AOCT of all five Chinese reference cities with a maximum absolute difference of 2.01 °C (within 0.5 °C for three; Supplementary Table S2).

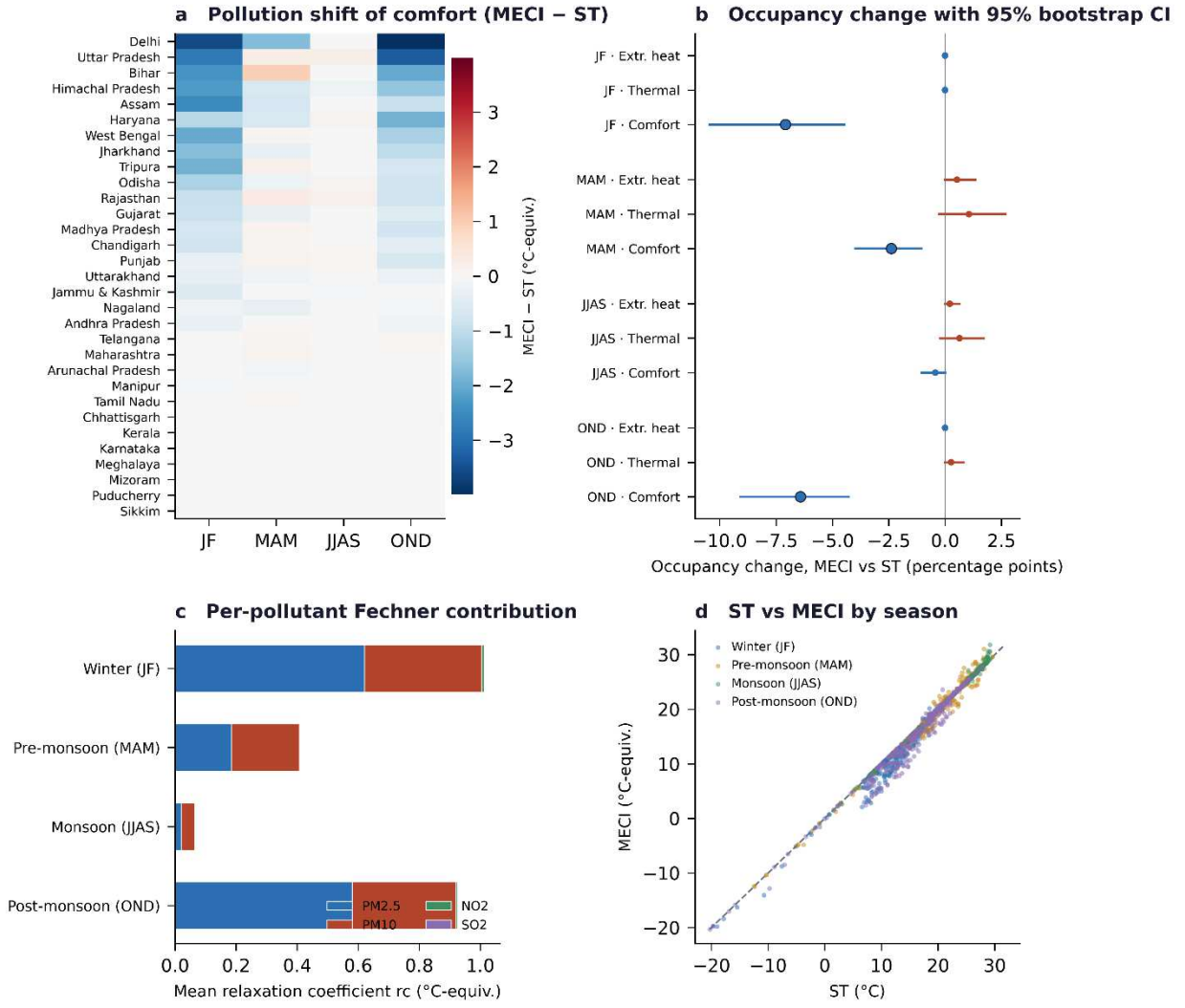


Figure 4 The India-calibrated pollution–comfort index. ***a***, *Mean comfort shift (MECI − ST) by state and IMD season.* ***b***, *Change in comfort-class occupancy under MECI relative to ST, nationally by season, with 95% bootstrap confidence intervals (filled markers, CI excluding zero).* ***c***, *Mean contribution of each pollutant's relaxation coefficient to the Fechner term frc, by season.* ***d***, *ST versus MECI by season with the 1:1 line; the relation is near-identity by construction, and the seasonal offsets quantify the pollution term. Relaxation coefficients are anchored to CPCB AQI/NAAQS breakpoints with rc ≥ 0 (Methods).*

Under the India-calibrated index, the pollution term frc behaves as regulatory logic requires: 54.8% of state-months — all four monthly pollutant means below the selected regulatory-reference anchors — are assigned zero modelled relaxation, and the national seasonal means are 1.03 °C-equivalent in winter and 0.91 in the post-monsoon against 0.06 in the monsoon, peaking at 3.6–4.0 °C-equivalent in Delhi's winter and post-monsoon (Fig. 4a). Particulate matter dominates the term (PM2.5 ≈ 55%, PM10 ≈ 31% of the winter mean), with NO_2 and SO_2 contributing negligibly because their monthly means rarely exceed the selected reference anchors (Fig. 4c). The comfort consequences concentrate in the cool seasons: relative to ST, the MECI significantly reduces Comfort-class occupancy by 7.1 percentage points in winter, 6.4 in the post-monsoon and 2.4 in the pre-monsoon, with corresponding gains in Cold discomfort (+4.1 and +3.2 points; 95% bootstrap CIs excluding zero in 5 of 28 class–season combinations; Fig. 4b), reflecting the formulation's convention that pollution deepens discomfort away from the optimum in either direction. The two indices otherwise track closely (seasonal regression slopes 1.01–1.05, $R^2 \geq 0.97$), with mean seasonal offsets of −0.98 °C-equivalent in winter and −0.84 in the post-monsoon (Fig. 4d).

Spatial dynamics of pollution-driven comfort loss

Mapping the seasonal comfort shift by state resolves when and where the pollution term bites (Fig. 5). The burden is overwhelmingly a cool-season, Indo-Gangetic phenomenon: in winter, 15 of 23 assessable states show a significant shift, all toward deeper cold-side discomfort, reaching −3.6 °C-equivalent in Delhi, and the post-monsoon repeats the pattern (14 of 26 states significant, Delhi −4.0, Uttar Pradesh −3.3 °C-equivalent), with the significant corridor running continuously from Punjab and Haryana through Uttar Pradesh and Bihar to West Bengal and Assam. The monsoon map is almost blank — washout holds every state's mean shift within ±0.23 °C-equivalent — while the pre-monsoon marks the seasonal turning point at which the burden changes sign: in Bihar, Punjab, Maharashtra and Telangana, where temperatures already exceed the comfort optimum, pollution adds significantly to warm-side discomfort (up to +0.9 °C-equivalent). The spatial contrast with the meteorology-only view is the central message of the figure: states whose thermal climates are indistinguishable (Fig. 3) separate sharply once the pollution dimension is admitted, and the separation follows India's emission geography rather than its thermal geography.

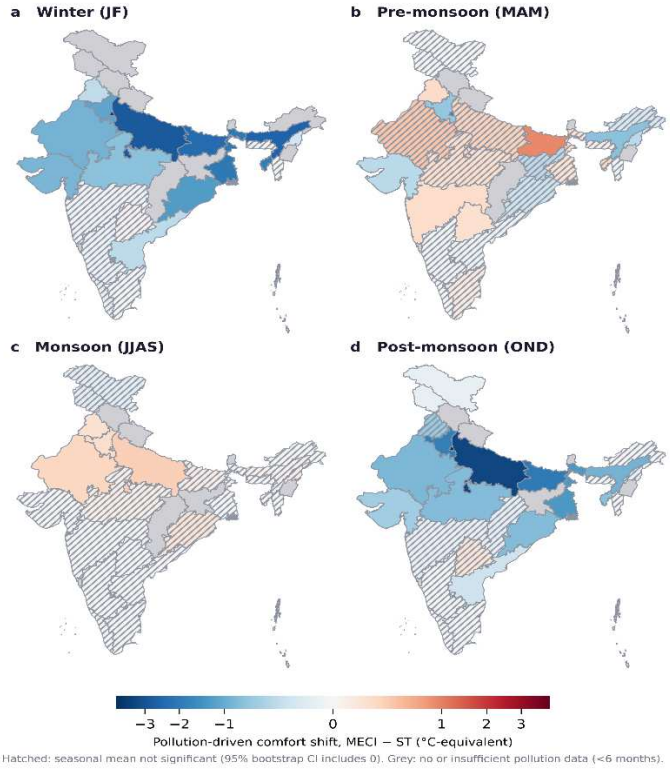


Figure 5 Seasonal geography of the pollution-driven comfort shift, 2016–2023. *State-mean comfort shift (MECI − ST, °C-equivalent) for the four IMD seasons:* ***a****, winter (JF);* ***b****, pre-monsoon (MAM);* ***c****, monsoon (JJAS);* ***d****, post-*

monsoon (OND). Negative values (blue) denote pollution deepening cold-side discomfort; positive values (red) added warm-side discomfort. Colour scale is square-root-stretched about zero for legibility of small shifts. Hatching, seasonal mean not significant (95% bootstrap CI includes zero); grey, no or insufficient pollution data (<6 months). Ladakh is displayed with Jammu & Kashmir, whose monitoring record predates the 2019 bifurcation.

A statistical persistence extrapolation indicates how this geography would evolve if NCAP-era pollutant trends continued (Supplementary Fig. S2). Projected to 2030, the annual burden declines in nine of fourteen projectable cohort states — significantly so, beyond the bootstrap uncertainty of the trend itself, only in Delhi (1.94 → 1.22 °C-equivalent) and Uttar Pradesh (0.95 → below the national-standard anchors) — while rising in Haryana (1.00 → 1.42), Maharashtra and Tamil Nadu, whose particulate trends point upward. We emphasise that this is a quantitative extrapolation under a single stated assumption of linear trend persistence, not an attribution or a climate projection, and that a projected burden of zero denotes concentrations below Indian national standards, which remain severalfold above WHO guidelines.

Dual exposure, population burden and alignment with SDG performance

Because neither UTCI nor an air-quality index alone can see the joint condition (Fig. 2), we classified every state-month on two distinct axes: UTCI thermal tier (cold side <9 °C; no stress 9–26 °C; heat stress >26 °C) and pollution tier from the India-calibrated Fechner term (clean, frc = 0; elevated, 0 < frc ≤ 1; high, frc > 1), the latter inheriting regulatory meaning from its NAAQS anchoring (Fig. 6). The joint distribution is strongly seasonal: the monsoon is India's clean-comfortable window (70% of state-months in the clean/no-stress cell), whereas the post-monsoon and winter concentrate the worst combinations — 21% and 13% of national state-months respectively fall in the high-pollution/cold-side cell, and a further 9–22% are thermally "comfortable" months carrying high pollution (Fig. 6a). That last cell matters: it s the modal condition of Uttar Pradesh, whose most frequent state is high pollution under no thermal stress — months a biometeorological index would certify as benign. Compound exposure — monthly pollutant means above the selected reference anchors coinciding with thermal conditions outside the no-stress band — occupies 48% of all months in Delhi, 43% in Uttar Pradesh, 41% in Haryana and 40% in Punjab (Fig. 6b, c).

Weighting by gridded population (1.288 billion in 24 eligible states/territories from 1.40 billion across the mapped areas; Methods) converts occupancy into burden: 2.98 billion person-months per year are spent under compound exposure across eligible states, led by Uttar Pradesh (1.21 billion, 41% of the total), Bihar (0.46 billion) and Rajasthan (0.36 billion) (Fig. 6d). Set against the 4.43 billion person-months of thermal stress that a UTCI-only assessment would register, two-thirds of India's thermal-stress exposure carries a concurrent pollution burden that the thermal index cannot see — and the comparison excludes entirely the high-pollution months inside the comfort band.

Finally, the burden aligns with states' sustainability performance in a specific way. The annual mean pollution-comfort burden correlates strongly and negatively with SDG 13 (Climate Action) scores in the 2023–24 SDG India Index (Spearman $r = -0.74$, $p < 0.001$, $n = 27$ states), but not with SDG 11 (Sustainable Cities; $r = -0.09$, $p = 0.64$) or SDG 7 (Clean Energy; $r = +0.10$, $p = 0.64$), and only weakly with the composite index ($r = -0.34$, $p = 0.08$) (Fig. 7). The burden thus tracks climate-action performance specifically, rather than urbanisation or energy access. These are state-level ecological associations and support a framing, not a causal claim.

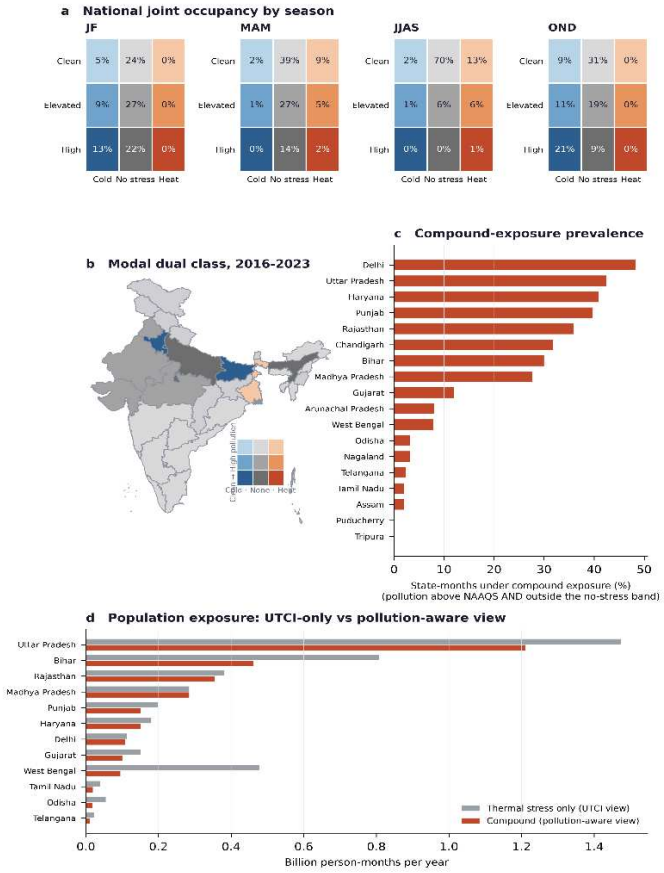


Figure 6 Dual-exposure classification and population burden, 2016–2023. ***a****, National joint occupancy of pollution tier (rows) × UTCI thermal tier (columns) by IMD season.* ***b****, Modal joint class per state (bivariate colour key inset).* ***c****, Fraction of state-months under compound exposure (pollution above national standards and thermal conditions outside the 9–26 °C no-stress band).* ***d****, Population exposure: person-months per year registered by a UTCI-only assessment (grey) versus under compound exposure (red); population from a 2020 gridded density surface aggregated to states (Methods). States with fewer than 24 classified months are excluded (grey).*

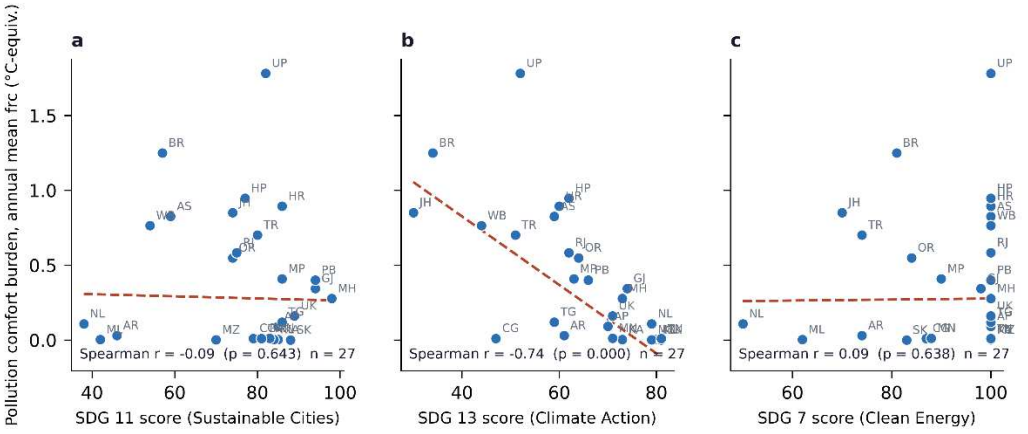


Figure 7 Pollution-comfort burden versus state SDG performance. *Annual mean Fechner burden frc per state against 2023–24 SDG India Index scores for* ***a****, SDG 11;* ***b****, SDG 13;* ***c****, SDG 7. Dashed lines, Theil–Sen fits; annotations give Spearman rank correlations. Union territories, ranked separately by NITI Aayog, are excluded (n = 27 states).*

Discussion

This study asked what air pollution does to outdoor thermal comfort at the scale of a subcontinent, and its answer rests on three results that together reframe how compound heat–pollution exposure should be measured in India. First, pollutant anomalies show no statistically detectable residual association with UTCI at monthly state scale once shared seasonality is removed, whether interrogated with two-way fixed-effects panel models under cluster-robust inference or with gradient-boosted learners validated out-of-state — the latter not merely failing to find a pollution signal but losing predictive skill when pollutant features are admitted, indicating no additional predictive benefit at this scale. Second, the published MECI index integrating the two dimensions does not survive transfer unmodified: below its WHO-2005 calibration interval, the Fechner terms of the MECI extrapolate into unbounded "comfort bonuses", a failure that could not have surfaced in the polluted Chinese cities where the index was built[55] and that was exposed here only by India's clean northeastern and Himalayan monitoring records. Third, once recalibrated to Indian regulatory anchors, the index characterises a model-defined compound burden with sharp structure — a winter and post-monsoon phenomenon of the Indo-Gangetic Plain, totalling 2.98 billion person-months annually, with Uttar Pradesh alone contributing two-fifths — and the dual-exposure classification built on it identifies, as the modal condition of India's most populous state, a category no operational index can see: thermally benign months under heavy pollution.

The absence of a detectable monthly-scale association deserves emphasis and sits, at first sight, in tension with the physical literature. Aerosol–radiation modelling shows pollution altering perceived heat non-monotonically — moderate optical depths raising physiological equivalent temperature through enhanced diffuse radiation, very heavy loading suppressing it[52] — and city-scale machine-learning attribution finds pollutant–UTCI associations that reverse between day and night and differ across climate zones,[54] while epidemiological work interprets ozone as a partial mediator of heat–mortality relationships.[13,60,61] Monthly means may obscure these opposing sub-daily pathways: the raw seasonal correlations we observe (reaching −0.8 in the stagnant post-monsoon) are the signature of shared meteorology, not of pollution influencing comfort, and they collapse under deseasonalisation. A perceptual pathway may also operate at a given thermal state, as published comfort-vote campaigns report worse comfort in polluted air.[53] The MECI framework is therefore an exposure-perception construct, not an energy-balance correction, and our recalibration bounds it accordingly: the model zero point is anchored to regulatory thresholds with established policy meaning,[62] the modelled relaxation term is floored at zero below the reference anchors rather than extrapolated into benefit, and the near-identity regression between ST and the recalibrated MECI (seasonal slopes 1.01–1.05) confirms that the pollution term acts as a seasonal offset on an otherwise unchanged thermal signal rather than distorting it. Two inherited design choices still warrant scrutiny. The convention that pollution deepens discomfort on the cold side as well as the warm[55] drives our winter results; it is perceptually plausible — haze, airway irritation and light attenuation all degrade the experience of cold outdoor air, and the respiratory burden of polluted Indian winters is well documented[33,38] — but it has not been validated with Indian comfort votes, and the survey designs that could do so[53] have no Indian counterpart. And anchoring "zero burden" to national standards severalfold above WHO guidelines[62] makes these modelled burden estimates conditional on the choice of national rather than stricter health-based reference thresholds.

The methodological finding merits a statement in its own right, because it generalises beyond this index. Perception-based environmental indices calibrated on bounded stimulus intervals fail silently outside those intervals: the logarithmic form that makes Fechner's law attractive within its calibration range[57,58] guarantees unbounded extrapolation outside it, and any transfer of such an index to a cleaner (or dirtier) environment requires re-anchoring to locally meaningful thresholds — for which, we suggest, regulatory breakpoints are the natural choice, since they carry governance meaning, are maintained by national agencies, and render the index's zero point auditable. Our India-calibrated coefficients, derivation and validation against the original study's published reference values are provided in full so that the same procedure can be repeated for any jurisdiction's standards.

The dual-exposure classification converts these methodological choices into a public-health instrument, and its most consequential output is the blind-spot category. Indian heat action planning activates on thermal thresholds; air-quality response activates on AQI categories; nothing activates on their conjunction — a gap mirrored in high-income settings, where heat warnings and air-quality indices operate on separate

triggers despite rising co-exposure[17,63,64] and where joint-hazard communication is only beginning to be designed.[65] Our results align with the convergent argument from the ozone direction — that heatwave governance must incorporate air-quality response[39] — and extend it: the conjunction needing management in India is not only the heatwave–ozone episode but the cold-season particulate peak coinciding with, and modelled as deepening, winter discomfort across the Indo-Gangetic Plain. The alignment of the comfort burden with SDG 13 scores specifically — rather than with urbanisation (SDG 11) or energy access (SDG 7) — suggests that climate-action capacity and modelled pollution-comfort outcomes may share state-level contextual determinants; this is an ecological association that invites, but cannot establish, causal interpretation, and disentangling it would require the quasi-experimental policy-evaluation designs long used in air-quality economics[66] and recently applied to Indian interventions.[35,37]

The persistence projection sharpens the policy reading without overclaiming. If NCAP-era pollutant trends continue, the comfort burden declines materially in Delhi and falls below national-standard anchors in Uttar Pradesh by 2030 — yet rises in Haryana, whose particulate trajectory points upward. The projected decline is thus conditional on continued state-specific trends, not a predicted national outcome, consistent with assessments that NCAP progress is real but uneven[34,36] and with evidence that recent improvements have been distributed unequally.[38] We stress the projection's single governing assumption — linear trend persistence — and its deliberate exclusions: no climate-model input, because scenario meteorology cannot supply the pollutant concentrations the index requires, and a stationary thermal baseline, because our own trend analysis resolves none over the study window. A projected burden of zero therefore denotes monthly means below the selected regulatory-reference anchors, not clean air by international criteria.[62] Extension to future climates is a staged problem that the two-axis design makes explicit: ensemble meteorology can project the thermal axis,[28] the pollution axis requires scenario concentration pathways, and their combination — together with the inequity dimension that compound-exposure projections emphasise[8,67] — is the natural sequel to this work.

Several limitations bound the results. Monthly state-level resolution compresses extremes — no monthly-mean UTCI in our panel exceeds the moderate-heat threshold, so absolute heat-stress frequencies require sub-daily analysis[47] — and the state medians represent each state's monitored, urban-biased environment rather than a true area average, a general limitation of regulatory networks[31,32] that weighs most heavily on the seven states served by a single station. Ozone, absent from our records, is precisely the pollutant that heatwaves amplify,[39,40] so the warm-season burden is likely underestimated; the formulation accepts an ozone term the moment monitoring data permit. The population-exposure accounting weights occupancy, not dose–response: converting person-months of compound exposure into attributable outcomes requires the interaction epidemiology now maturing around joint temperature–PM2.5 designs,[6,14,16–18] whose vulnerability dimension — age, socioeconomic position, outdoor occupation — is documented elsewhere but unaddressed here.[68,69] And the perceptual foundation of the Fechner term, while psychophysically grounded,[57,58] awaits Indian field validation; a national comfort-vote campaign spanning the pollution gradient from the Indo-Gangetic winter to the northeastern monsoon would both test the cold-side convention and refine the India-specific anchors, and we identify it as the single most valuable measurement this field could add.

What this study establishes meanwhile is the accounting framework such measurements would refine. Pollution and thermal stress in India are represented by distinct exposure measures, jointly experienced and separately governed; their conjunction occupies nearly half the year in the states where a sixth of humanity lives; and the 2.98 billion person-months on which they coincide each year are currently visible to no operational index. Making that burden visible — in a form anchored to the regulatory thresholds governments already enforce — is the contribution this work offers to the integration of air-quality and heat governance that both research directions, heat-to-pollution[39] and pollution-to-comfort, now independently demand.

Methods

Study area and period. The study covered the states and union territories of mainland India over 2016–2023, analysed at monthly resolution on a state-level spatial framework. This framework was chosen to match the coarsest common support of the regulatory air-quality network and the reanalysis-derived thermal fields, enabling a single consistent panel of 3,032 valid state-months across 32 administrative units. The year 2024 was excluded in its entirety because the source records contained only partially reported months. Administrative boundaries were used for geographical visualisation and for aggregation of gridded ancillary data; Ladakh was displayed jointly with Jammu & Kashmir, whose monitoring record predates the 2019 bifurcation. Seasons follow the India Meteorological Department convention: winter (January–February, JF), pre-monsoon (March–May, MAM), monsoon (June–September, JJAS) and post-monsoon (October–December, OND).

Air-quality observations and quality control. Monthly mean concentrations of $PM_{2.5}$, PM_{10}, NO_2 and SO_2 were compiled from 423 continuous ambient air-quality monitoring stations of the Central Pollution Control Board (CPCB) network, distributed across 31 states and union territories. Goa has no station in the record, and seven states are served by a single station; these were retained but flagged in all diagnostics. Stations were assigned to states through their network codes, and the state–month concentration of each pollutant was computed as the median across reporting stations, a choice that resists single-station outliers. Two quality-control rules were applied before aggregation. First, any station-year block in which a pollutant exhibited at most two unique values across six or more reported months was treated as imputed and masked. Second, for trend estimation a 14-state cohort was defined, comprising states with at least 60% monthly $PM_{2.5}$ coverage whose records begin no later than 2017; this reduces sensitivity to artefacts from the rapid post-2017 expansion of the monitoring network. As an additional sensitivity analysis, all $PM_{2.5}$ trends were recomputed using only the 61 stations that reported continuously from 2017 or earlier, and broadly similar cohort-level patterns were obtained, although state-level trend directions did not agree universally.

Thermal and meteorological data. Monthly state-mean near-surface air temperature and the Universal Thermal Climate Index (UTCI) were derived from the ERA5 reanalysis[70] and its thermal-comfort extension,[47,48] averaged over state masks. Forty-eight monthly UTCI values below 220 K, confined to the high-Himalayan averages of Jammu & Kashmir and Himachal Pradesh where the UTCI polynomial approximation leaves its validity domain, were masked; state means over such terrain represent area averages rather than inhabited-valley conditions, and are interpreted accordingly throughout. The meteorological inputs to the somatosensory-temperature calculation — monthly mean relative humidity, 10-m wind speed and total precipitation — were extracted from ERA5 on the same state masks. Relative humidity was obtained from the 2-m air temperature T and dewpoint T_d (°C) through the Magnus formulation,

$$\mathrm{RH} = 100\,\frac{e(T_d)}{e(T)}, \qquad e(x) = \exp\left(\frac{17.625\,x}{243.04 + x}\right). \qquad (1)$$

Wind speed was computed from the monthly mean wind components, a standard approximation that modestly underestimates the mean of instantaneous speeds; this choice is applied uniformly and is therefore neutral to all comparative results.

Trend analysis. Monotonic trends were assessed with the seasonal Mann–Kendall test,[71,72] in which the test statistic is computed within each calendar month and summed across the year, so that the seasonal cycle cannot masquerade as trend. For a given state, calendar month m and variable with annual values $x_1, \ldots, x_n$, the monthly statistic is

$$S_m = \sum_{i<j} \mathrm{sgn}\left(x_j - x_i\right), \qquad (2)$$

where $\mathrm{sgn}(\cdot)$ takes the values 1, 0 and −1 for positive, zero and negative arguments. Its variance, corrected for tied values, is

$$\mathrm{Var}(S_m) = \frac{n(n-1)(2n+5) - \sum_p t_p\,\left(t_p-1\right)\left(2t_p+5\right)}{18}, \qquad (3)$$

where t_p is the number of ties in the p-th tied group. The seasonal statistic and its variance sum over the twelve calendar months,

$$S = \sum_{m=1}^{12} S_m\,, \qquad \mathrm{Var}(S) = \sum_{m=1}^{12} \mathrm{Var}\,(S_m), \qquad (4)$$

and significance is evaluated through the continuity-corrected standard normal deviate

$$Z = \frac{S - \mathrm{sgn}(S)}{\sqrt{\mathrm{Var}(S)}}. \qquad (5)$$

Trend magnitudes are reported as seasonal Sen's slopes,[73]

$$\beta = \mathrm{median}\left(\frac{x_j - x_i}{t_j - t_i}\right), \quad i < j, \qquad (6)$$

where the median is taken over all pairs of years $i < j$ within the same calendar month, pooled across months, in units per year. Throughout, significance is reported at $p < 0.05$.

Association analysis. All association tests operate on state–month anomalies, defined for any variable y in state s, calendar month m and year t as

$$y'(s,m,t) = y(s,m,t) - \bar{y}(s,m), \qquad (7)$$

where $\bar{y}(s,m)$ is the 2016–2023 mean of y for that state and calendar month; this removes both the seasonal cycle and fixed geography. Raw Spearman rank correlations and Pearson correlations on anomalies were computed by season for each pollutant (Fig. 2). The panel regression model is

$$\mathrm{UTCI}'(s,m,t) = \alpha + \beta_P\,\frac{\mathrm{PM}_{2.5}{}'(s,m,t)}{10} + \gamma_t + \varepsilon(s,m,t), \qquad (8)$$

where β_P is the UTCI response per 10 μg m^{-3} $PM_{2.5}$ anomaly, γ_t are year fixed effects and ε is the error term. The model was estimated by ordinary least squares with CR1 cluster-robust standard errors clustered by state, with inference on a t-distribution with $G-1$ degrees of freedom for $G = 14$ clusters; a second specification added NO_2 anomalies, and season-stratified models repeated the estimation within each IMD season. As a nonlinearity check (Supplementary Fig. S1), gradient-boosted regression trees (400 iterations, maximum depth 4, learning rate 0.05) were fitted to UTCI anomalies from the four pollutant anomalies, seasonal harmonics and year, and validated by five-fold grouped cross-validation with states as groups, so that all reported skill is out-of-state. The contribution of pollution was summarised as the difference in cross-validated R^2 between the full model and an otherwise identical model refitted without pollutant features, with permutation importance evaluated on held-out folds only.

Somatosensory temperature. The somatosensory temperature (ST) follows the golden-section formulation.[55,56] The actual optimum comfort temperature of a state in month M is

$$\mathrm{AOCT} = 22.7[1 - 0.3\sin(\varphi - 23.5)] - |0.3\cos(15^\circ(M-1))| - 2\tan\left(\frac{H}{100}^\circ\right), \qquad (9)$$

where φ is the representative latitude (degrees), H the representative elevation (m), and the latitude term is evaluated in radians, as in the original implementation: this convention, rather than the nominal degree reading, reproduces the published mean AOCT of all five Chinese reference cities with a maximum absolute difference of 2.01 °C, and within 0.5 °C for three of them (Supplementary Table S2). With t_a the air temperature (°C), rh the relative humidity (fraction), v the wind speed (m s^{-1}) and rh_s the optimum humidity (0.5, or 0.618 in months with more than 1 mm precipitation), ST is

$$\mathrm{ST} = t_a + a\left[e^{\,0.05\,(t_a-\mathrm{AOCT})(rh-rh_s)} - 1\right] - 0.03\,(t_a - \mathrm{AOCT})\,v, \qquad t_a \geq \mathrm{AOCT}, \qquad (10)$$

$$\mathrm{ST} = t_a - a\left[e^{\,0.013\,(\mathrm{AOCT}-t_a)(rh-rh_s)} - 1\right] - 0.01\,(\mathrm{AOCT} - t_a)\,v, \qquad t_a < \mathrm{AOCT}, \qquad (11)$$

where $a = 36.75\,(1 - 0.618) \approx 14.04$.

Fechner relaxation coefficients and the MECI. The perceived contribution of each pollutant follows Fechner's law of logarithmic stimulus perception,[57,58] expressed as a relaxation coefficient

$$rc_i = k_i \log_{10} C_i + c_i, \qquad (12)$$

where C_i is the concentration of pollutant i (μg m^{-3}) and the coefficients k_i and c_i are fixed by two boundary conditions anchoring the perceived sensation to zero at a lower concentration limit and to unity at an upper limit:

$$0 = k_i \log_{10} C_{i,\mathrm{low}} + c_i, \qquad 1 = k_i \log_{10} C_{i,\mathrm{high}} + c_i. \qquad (13)$$

The influence function sums the available pollutant terms,

$$f_{rc} = \sum_i r\, c_i, \qquad (14)$$

and the Meteorology and Environment Comfort Index follows the original convention[55] that pollution displaces perceived conditions away from the optimum on either side:

$$\mathrm{MECI} = \begin{cases} \mathrm{ST} + f_{rc}, & t_a \geq \mathrm{AOCT}, \\ \mathrm{ST} - f_{rc}, & t_a < \mathrm{AOCT}. \end{cases} \qquad (15)$$

Both indices are classified on the published seven-standard comfort scale through the optimum comfort index$\mathrm{OCI} = 22.7 - \mathrm{AOCT}$.[55]

India recalibration. The original coefficients anchor C_{low} and C_{high} to the WHO-2005 guideline and its nearest interim target.[55] Below C_{low}, equation (12) extrapolates without bound into negative sensation, which we identify as a transfer artefact (Results); accordingly, all coefficients were re-derived with Indian regulatory anchors and the relaxation coefficients floored at zero,

$$rc_i = \max[0,\ k_i \log_{10} C_i + c_i], \qquad (16)$$

so that monthly means below the selected regulatory-reference anchors contribute zero modelled relaxation rather than a perceived benefit. The anchors place C_{low} at the CPCB Air Quality Index "Satisfactory" bound — which coincides with the National Ambient Air Quality Standards 24-hour value but is used as a modelling reference for monthly means[74,75] — and C_{high} at the next CPCB AQI breakpoint: 60→90 μg m^{-3} for $PM_{2.5}$, 100→250 for PM_{10}, 80→180 for NO_2 and 80→380 for SO_2. The resulting coefficient set (for example, $rc_{\mathrm{PM}_{2.5}} = 5.679 \log_{10} C - 10.098$) is reported in Supplementary Table S1. The original unclipped WHO-anchored calibration was retained as a sensitivity configuration, and a concentration floor of 1 μg m^{-3} was applied before taking logarithms.

Spatial analysis and uncertainty quantification. State–season mean comfort shifts, $\mathrm{MECI} - \mathrm{ST}$, carry 95% confidence intervals obtained by bootstrap resampling of the constituent months within each state–season ($B = 1{,}000$ resamples, fixed seed); state–seasons with fewer than six valid months are displayed as insufficient data. National changes in comfort-class occupancy between ST and MECI were evaluated with the same bootstrap applied to state-months within each season, and a change was considered significant when its 95% interval excluded zero.

Dual-exposure classification. Each state-month was classified jointly on two axes. The thermal axis partitions monthly-mean UTCI into cold side (<9 °C), no thermal stress (9–26 °C) and heat stress (>26 °C), following the standard UTCI assessment scale;[43–46] classes above moderate heat are unreachable by monthly means, which compress sub-monthly extremes, and the classification is interpreted at monthly resolution only. The pollution axis partitions the India-calibrated influence function into clean ($f_{rc} = 0$,

monthly pollutant means below the selected reference anchors), elevated ($0 < f_{rc} \leq 1$) and high ($f_{rc} > 1$), inheriting regulatory meaning from the NAAQS anchoring. Compound exposure denotes the joint condition of monthly pollutant means above the selected reference anchors and thermal conditions outside the no-stress band; it is a model-defined state-month category. States with fewer than 24 classified months were excluded from state-level summaries.

Population-exposure weighting. Human population was obtained from a gridded population-density surface for 2020 at approximately 1-km resolution.[76] Density was converted to persons per cell using latitude-dependent cell areas,

$$A(\varphi) = (111.32\,\Delta\varphi)(111.32\cos\varphi\,\Delta\lambda), \qquad (17)$$

where $\Delta\varphi$ and $\Delta\lambda$ are the cell dimensions in degrees, and the resulting person counts were aggregated onto an approximately 0.085° grid and assigned to states by point-in-polygon evaluation against the administrative boundaries, preserving population totals (1.40 billion across the mapped areas; 1.288 billion in the 24 states/territories with at least 24 classified months). The population burden of any exposure class was then computed as

$$\mathrm{PM}_{\mathrm{yr}}(s) = \mathrm{Pop}(s)\, f_{\mathrm{class}}(s) \times 12, \qquad (18)$$

where $f_{\mathrm{class}}(s)$ is the fraction of state s's classified months in that class and $\mathrm{PM}_{\mathrm{yr}}$ is expressed in person-months per year.

Association with SDG performance. State scores for SDG 7, SDG 11, SDG 13 and the composite index were taken from the SDG India Index 2023–24.[77] Union territories are ranked separately by NITI Aayog and were excluded, leaving 27 states. Associations between the annual mean burden f_{rc} and each score were quantified by Spearman rank correlation, with Theil–Sen fits shown for display; these are state-level ecological associations and are interpreted as such.

Persistence projection. The near-term projection holds each cohort state's monthly concentration climatology, computed over the 2021–2023 baseline, and advances it to 2030 under the state's seasonal Sen's slope,

$$C_i(m, 2030) = \bar{C}_i(m) + \beta_i\,(2030 - 2022), \qquad (19)$$

where $\bar{C}_i(m)$ is the baseline climatology of pollutant i in calendar month m and β_i the Sen's slope from equation (6); projected concentrations are floored at 1 μg m^{-3}. The projected influence function and burden were recomputed through equations (12)–(16). Confidence intervals were obtained by re-estimating the slopes under bootstrap resampling of the contributing years ($B = 500$ resamples). The projection embodies a single stated assumption — linear persistence of 2016–2023 trends — with no climate-model input and a stationary thermal baseline, the latter consistent with the absence of resolvable UTCI trends over the study window; a projected burden of zero denotes monthly means below the selected regulatory-reference anchors, not clean air by international criteria.[62]

Statistics and software. All analyses were implemented in Python using NumPy, pandas, SciPy, Matplotlib and scikit-learn. Every stochastic procedure carries a fixed random seed, and the complete pipeline — panel construction, quality control, statistics, figures and diagnostic tables — regenerates deterministically from the two source data files through a documented sequence of scripts, each of which writes its figure, its underlying data and a provenance record.

Data availability

The input datasets are available from the public sources cited in the Methods section: Central Pollution Control Board continuous ambient monitoring records (https://airquality.cpcb.gov.in), ERA5 and ERA5-HEAT fields from the Copernicus Climate Data Store, the WorldPop gridded population surface (www.worldpop.org) and SDG India Index scores from NITI Aayog. The processed state–month panel and the source data underlying the figures, tables and statistical analyses will be supplied in a ZIP archive accompanying the submission for confidential peer review. Public archival details will be included in the manuscript before publication.

Code availability

The complete analysis pipeline — panel construction and quality control, trend and association statistics, the India-calibrated index computation, the dual-exposure classification, population-exposure weighting and all figure-generation scripts, each writing its figure together with its underlying data and a provenance record — will be supplied in a ZIP archive accompanying the submission for confidential peer review. The pipeline is deterministic, with fixed random seeds, and regenerates every result from the source data. Public archival details and applicable licence terms will be included in the manuscript before publication.

Acknowledgements

This research received no specific funding. The authors thank the Central Pollution Control Board and the Copernicus Climate Change Service for open provision of the observational and reanalysis records used in this study. Generative-AI assistance was used in code development and manuscript preparation, under close supervision of the authors, and was not used in conceptualisation, analysis or interpretation of results

Author contributions

P.S.H.P. conceived the study, designed the India recalibration and the dual-exposure classification, assembled and quality-controlled the datasets, performed all analyses, generated the figures and tables, interpreted the results and drafted the manuscript. A.N.V.S. supervised the research and reviewed and corrected the manuscript. Both authors approved the final manuscript.

Competing interests

The authors declare no competing interests.

Ethics

Ethics approval and informed consent were not required: the study involved no human participants, identifiable individual-level information, biological specimens or experimental intervention.

References

1. Zscheischler, J. et al. A typology of compound weather and climate events. *Nat. Rev. Earth Environ.* **1**, 333–347 (2020).
2. Brett, L. et al. Review article: The growth in compound weather and climate event research in the decade since SREX. *Nat. Hazards Earth Syst. Sci.* **25**, 2591–2611 (2025).
3. AghaKouchak, A. et al. Climate extremes and compound hazards in a warming world. *Annu. Rev. Earth Planet. Sci.* **48**, 519–548 (2020).
4. Marlier, M. E., Connolly, R., Ma, Y., Jerrett, M. & Benmarhnia, T. Compound climate exposures and public health: a synthesis of research and future directions. *Annu. Rev. Public Health* **47**, 305–323 (2026).
5. Ebi, K. L. Understanding the risks of compound climate events and cascading risks. *Dialogues Clim. Change* **2**, 33–37 (2025).
6. Chen, D., Zahid, M. & Qiu, M. Characterizing the compound extreme temperature and PM2.5 pollution events: a multi-country analysis. *GeoHealth* **10**, e2025GH001763 (2026).
7. Coffel, E. D., Horton, R. M. & de Sherbinin, A. Temperature and humidity based projections of a rapid rise in global heat stress exposure during the 21st century. *Environ. Res. Lett.* **13**, 014001 (2018).
8. Ban, J., Lu, K., Wang, Q. & Li, T. Climate change will amplify the inequitable exposure to compound heatwave and ozone pollution. *One Earth* **5**, 677–686 (2022).
9. Anenberg, S. C., Haines, S., Wang, E., Nassikas, N. & Kinney, P. L. Synergistic health effects of air pollution, temperature, and pollen exposure: a systematic review of epidemiological evidence. *Environ. Health* **19**, 130 (2020).
10. Grigorieva, E. & Lukyanets, A. Combined effect of hot weather and outdoor air pollution on respiratory health: literature review. *Atmosphere* **12**, 790 (2021).

11. Analitis, A. et al. Effects of heat waves on mortality: effect modification and confounding by air pollutants. *Epidemiology* **25**, 15–22 (2014).
12. Lee, W. et al. Synergic effect between high temperature and air pollution on mortality in Northeast Asia. *Environ. Res.* **178**, 108735 (2019).
13. Shi, W. et al. Modification effects of temperature on the ozone–mortality relationship: a nationwide multicounty study in China. *Environ. Sci. Technol.* **54**, 2859–2868 (2020).
14. Xu, R. et al. Extreme temperature events, fine particulate matter, and myocardial infarction mortality. *Circulation* **148**, 312–323 (2023).
15. Castro, E. et al. Interactive effects between extreme temperatures and PM2.5 on cause-specific mortality in thirteen US states. *Environ. Res. Lett.* **20**, 014011 (2025).
16. Chen, C., Schwarz, L., Rosenthal, N., Marlier, M. E. & Benmarhnia, T. Exploring spatial heterogeneity in synergistic effects of compound climate hazards: extreme heat and wildfire smoke on cardiorespiratory hospitalizations in California. *Sci. Adv.* **10**, eadj7264 (2024).
17. Coker, E. S., Cleland, S. E., McVea, D., Stafoggia, M. & Henderson, S. B. The synergistic effects of PM2.5 and high temperature on community mortality in British Columbia. *npj Clean Air* **1**, 15 (2025).
18. Zhang, Y. et al. Compound effects of extreme heat and wildfire-PM2.5 air pollution on child hospitalizations in multiple countries. *Nat. Health* **1**, 1129–1140 (2026).
19. Schnell, J. L. & Prather, M. J. Co-occurrence of extremes in surface ozone, particulate matter, and temperature over eastern North America. *Proc. Natl Acad. Sci. USA* **114**, 2854–2859 (2017).
20. Zhang, H., Wang, Y., Park, T. W. & Deng, Y. Quantifying the relationship between extreme air pollution events and extreme weather events. *Atmos. Res.* **188**, 64–79 (2017).
21. Leffel, J., Wang, C., Hu, X.-M., Feron, S. & Henry, S. Cities as hotspots of compound heat and fine particulate matter pollution: a 23-year urban–rural comparison across the United States. *Environ. Res.* **285**, 122508 (2025).
22. Rosenthal, N., Benmarhnia, T., Ahmadov, R., James, E. & Marlier, M. E. Population co-exposure to extreme heat and wildfire smoke pollution in California during 2020. *Environ. Res. Clim.* **1**, 025004 (2022).
23. Ratnam, J. V., Behera, S. K., Ratna, S. B., Rajeevan, M. & Yamagata, T. Anatomy of Indian heatwaves. *Sci. Rep.* **6**, 24395 (2016).
24. Rohini, P., Rajeevan, M. & Srivastava, A. K. On the variability and increasing trends of heat waves over India. *Sci. Rep.* **6**, 26153 (2016).
25. Singh, S., Mall, R. K. & Singh, N. Changing spatio-temporal trends of heat wave and severe heat wave events over India: an emerging health hazard. *Int. J. Climatol.* **41**, E1831–E1845 (2021).
26. Pai, D. S., Nair, S. & Ramanathan, A. N. Long term climatology and trends of heat waves over India during the recent 50 years (1961–2010). *Mausam* **64**, 585–604 (2013).
27. Shukla, K. K., Attada, R., Kumar, A., Kunchala, R. K. & Sivareddy, S. Comprehensive analysis of thermal stress over northwest India: climatology, trends and extremes. *Urban Clim.* **44**, 101188 (2022).
28. Kumar, R., Kuttippurath, J., Gopikrishnan, G. S., Kumar, P. & Varikoden, H. Enhanced surface temperature over India during 1980–2020 and future projections: causal links of the drivers and trends. *npj Clim. Atmos. Sci.* **6**, 164 (2023).
29. Watts, N. et al. The 2020 report of The Lancet Countdown on health and climate change: responding to converging crises. *Lancet* **397**, 129–170 (2021).
30. Kaur, R. & Pandey, P. Air pollution, climate change, and human health in Indian cities: a brief review. *Front. Sustain. Cities* **3**, 705131 (2021).
31. Guttikunda, S. & KA, N. Evolution of India's PM2.5 pollution between 1998 and 2020 using global reanalysis fields coupled with satellite observations and fuel consumption patterns. *Environ. Sci.: Atmos.* **2**, 1502–1515 (2022).
32. Dey, S. et al. A satellite-based high-resolution (1-km) ambient PM2.5 database for India over two decades (2000–2019): applications for air quality management. *Remote Sens.* **12**, 3872 (2020).

33. Krishna, B. et al. Daily nonaccidental mortality associated with short-term PM2.5 exposures in Delhi, India. *Environ. Epidemiol.* **5**, e167 (2021).
34. Centre for Research on Energy and Clean Air. *Tracing the Hazy Air 2025: Progress Report on National Clean Air Programme (NCAP)* (CREA, 2025).
35. Ganguly, T., Selvaraj, K. L. & Guttikunda, S. K. National Clean Air Programme (NCAP) for Indian cities: review and outlook of clean air action plans. *Atmos. Environ.: X* **8**, 100096 (2020).
36. Gopikrishnan, G. S. & Kuttippurath, J. Four years of National Clean Air Programme (NCAP) in Indian cities: assessment of the impact on surface ozone during 2018–2022. *Sustain. Cities Soc.* **101**, 105207 (2024).
37. Beig, G. et al. Quantifying the effect of air quality control measures during the 2010 Commonwealth Games at Delhi, India. *Atmos. Environ.* **80**, 455–463 (2013).
38. Kawano, A. et al. Improved daily PM2.5 estimates in India reveal inequalities in recent enhancement of air quality. *Sci. Adv.* **11**, eadq1071 (2025).
39. Sangeetha, P. & Kuttippurath, J. Heatwaves trigger severe surface ozone pollution in India: regional hotspots, trends and health effects. *npj Clean Air* **2**, 40 (2026).
40. Gopikrishnan, G. S., Ardra, T. S. & Kuttippurath, J. Exposure to surface ozone and its associated health effects and economic burden in India. *Glob. Transit.* **7**, 148–158 (2025).
41. Kumar, P., Chakraborty, A. & Sagar, A. K. Impact of heatwaves on air pollutants in major climatic zones of India. *Discov. Geosci.* **3**, 119 (2025).
42. Thom, E. C. The discomfort index. *Weatherwise* **12**, 57–61 (1959).
43. Höppe, P. The physiological equivalent temperature – a universal index for the biometeorological assessment of the thermal environment. *Int. J. Biometeorol.* **43**, 71–75 (1999).
44. Bröde, P. et al. Deriving the operational procedure for the Universal Thermal Climate Index (UTCI). *Int. J. Biometeorol.* **56**, 481–494 (2012).
45. Fiala, D., Havenith, G., Bröde, P., Kampmann, B. & Jendritzky, G. UTCI-Fiala multi-node model of human heat transfer and temperature regulation. *Int. J. Biometeorol.* **56**, 429–441 (2012).
46. Błażejczyk, K., Epstein, Y., Jendritzky, G., Staiger, H. & Tinz, B. Comparison of UTCI to selected thermal indices. *Int. J. Biometeorol.* **56**, 515–535 (2012).
47. Di Napoli, C., Barnard, C., Prudhomme, C., Cloke, H. L. & Pappenberger, F. ERA5-HEAT: a global gridded historical dataset of human thermal comfort indices from climate reanalysis. *Geosci. Data J.* **8**, 2–10 (2021).
48. Di Napoli, C., Hogan, R. J. & Pappenberger, F. Mean radiant temperature from global-scale numerical weather prediction models. *Int. J. Biometeorol.* **64**, 1233–1245 (2020).
49. Sen, J. & Nag, P. K. Effectiveness of human-thermal indices: spatio-temporal trend of human warmth in tropical India. *Urban Clim.* **27**, 351–371 (2019).
50. Kumar, P. & Sharma, A. Assessing the outdoor thermal comfort conditions of exercising people in the semi-arid region of India. *Sustain. Cities Soc.* **76**, 103366 (2022).
51. Kotharkar, R. & Dongarsane, P. Investigating outdoor thermal comfort variations across Local Climate Zones in Nagpur, India, using ENVI-met. *Build. Environ.* **249**, 111122 (2024).
52. Wai, K.-M. et al. Aerosol pollution and its potential impacts on outdoor human thermal sensation: East Asian perspectives. *Environ. Res.* **158**, 753–758 (2017).
53. Sun, T., Liu, X., Liu, X., Nan, K. & Bian, G. Interaction effects of outdoor thermal comfort and air pollution. *Sci. Rep.* **15**, 37549 (2025).
54. Huang, K. et al. The spatiotemporal dynamics of air pollutants and the Universal Thermal Climate Index in 370 Chinese cities. *Atmosphere* **16**, 1263 (2025).
55. Zhang, S. et al. Influence of air pollution on human comfort in five typical Chinese cities. *Environ. Res.* **195**, 110318 (2021).
56. Wang, S. et al. Human body comfortable degree computing method constructed based on golden section method. Chinese patent CN103106336A (2013).

689 57. Norwich, K. H. & Wong, W. Unification of psychophysical phenomena: the complete form of Fechner's
690 law. *Percept. Psychophys.* **59**, 929–940 (1997).
691 58. Portugal, R. D. & Svaiter, B. F. Weber–Fechner law and the optimality of the logarithmic scale. *Minds*
692 *Mach.* **21**, 73–81 (2011).
693 59. Nahid, S., Acharya, P., Kumar, K. & Kumar, R. P. Spatio-temporal dynamics of urban thermal-pollution
694 interactions in Delhi and its surrounding areas: a remote sensing and GAM modelling approach.
695 *Environ. Res.* **307**, 125366 (2026).
696 60. Alari, A. et al. The role of ozone as a mediator of the relationship between heat waves and mortality in
697 15 French urban areas. *Am. J. Epidemiol.* **192**, 949–962 (2023).
698 61. Bae, S., Lim, Y.-H., Oh, J. & Kwon, H.-J. Mediation of daily ambient ozone concentration on association
699 between daily mean temperature and mortality in 7 metropolitan cities of Korea. *Environ. Int.* **178**,
700 108078 (2023).
701 62. World Health Organization. *WHO Global Air Quality Guidelines: Particulate Matter (PM2.5 and PM10),*
702 *Ozone, Nitrogen Dioxide, Sulfur Dioxide and Carbon Monoxide* (WHO, 2021).
703 63. Masselot, P. et al. Excess mortality attributed to heat and cold: a health impact assessment study in
704 854 cities in Europe. *Lancet Planet. Health* **7**, e271–e281 (2023).
705 64. Khatana, S. A. M., Werner, R. M. & Groeneveld, P. W. Association of extreme heat with all-cause
706 mortality in the contiguous US, 2008–2017. *JAMA Netw. Open* **5**, e2212957 (2022).
707 65. Coker, E. S. et al. Climate change and health: rethinking public health messaging for wildfire smoke
708 and extreme heat co-exposures. *Front. Public Health* **12**, 1324662 (2024).
709 66. Davis, L. W. The effect of driving restrictions on air quality in Mexico City. *J. Polit. Econ.* **116**, 38–81
710 (2008).
711 67. Cleland, S. E., Paul, N., Coker, E. S. & Henderson, S. B. The co-occurrence of wildfire smoke and
712 extreme heat events in British Columbia, 2010–2022: evaluating spatiotemporal trends and inequities
713 in exposure burden. *ACS EST Air* **2**, 319–330 (2025).
714 68. Azzouz, M. et al. Does socioeconomic and environmental burden affect vulnerability to extreme air
715 pollution and heat? A case-crossover study of mortality in California. *J. Expo. Sci. Environ. Epidemiol.*
716 **35**, 294–302 (2025).
717 69. De Sario, M., Katsouyanni, K. & Michelozzi, P. Climate change, extreme weather events, air pollution
718 and respiratory health in Europe. *Eur. Respir. J.* **42**, 826–843 (2013).
719 70. Hersbach, H. et al. The ERA5 global reanalysis. *Q. J. R. Meteorol. Soc.* **146**, 1999–2049 (2020).
720 71. Mann, H. B. Nonparametric tests against trend. *Econometrica* **13**, 245–259 (1945).
721 72. Kendall, M. G. *Rank Correlation Methods* 4th edn (Charles Griffin, London, 1975).
722 73. Sen, P. K. Estimates of the regression coefficient based on Kendall's tau. *J. Am. Stat. Assoc.* **63**, 1379–
723 1389 (1968).
724 74. Central Pollution Control Board. *National Ambient Air Quality Standards* (CPCB, New Delhi, 2009).
725 75. Central Pollution Control Board. *National Air Quality Index: Final Report*. Control of Urban Pollution
726 Series CUPS/82/2014-15 (CPCB, New Delhi, 2014).
727 76. WorldPop. The spatial distribution of population density in 2020, India. WorldPop
728 https://doi.org/10.5258/SOTON/WP00674 (2020).
729 77. NITI Aayog. *SDG India Index 2023–24* (Government of India, New Delhi, 2024).

Supplementary Files

This is a list of supplementary files associated with this preprint. Click to download.

- npjCleanAirSupplementarySUBMISSIONFINAL.pdf